Micrometeorite Impacts in Beringian Mammoth Tusks and a Bison Skull

J.T. Hagstrum[1], R.B. Firestone[2], A. West[3], Z. Stefanka[4], Z. Revay[4]

[1]*U.S. Geological Survey, 345 Middlefield Road, Menlo Park, CA 94025, United States*
[2]*Lawrence Berkeley National Laboratory, Berkeley, CA 94720, United States*
[3]*GeoScience Consulting, Dewey, AZ, 86327, United States*
[4]*Institute of Isotopes, Budapest, H-1525, Hungary*

Abstract

We have discovered what appear to be micrometeorites embedded in seven late Pleistocene Alaskan mammoth tusks and a Siberian bison skull. The micrometeorites apparently shattered on impact leaving 2 to 5 mm hemispherical debris patterns surrounded by carbonized rings. Multiple impacts are observed on only one side of the tusks and skull consistent with the micrometeorites having come from a single direction. The impact sites are strongly magnetic indicating significant iron content. We analyzed several imbedded micrometeorite fragments from both tusks and skull with laser ablation inductively coupled plasma mass spectrometry (LA-ICP-MS) and X-ray fluorescence (XRF). These analyses confirm the high iron content and indicate compositions highly enriched in nickel and depleted in titanium, unlike any natural terrestrial sources. In addition, electron microprobe (EMP) analyses of a Fe-Ni sulfide grain (tusk 2) show it contains between 3 and 20 weight percent Ni. Prompt gamma-ray activation analysis (PGAA) of a particle extracted from the bison skull indicates ~0.4 mg of iron, in agreement with a micrometeorite ~1 mm in diameter. In addition, scanning electron microscope (SEM) images and XRF analyses of the skull show possible entry channels containing Fe-rich material. The majority of tusks (5/7) have a calibrated weighted mean ^{14}C age of 32.9 ± 1.8 ka BP, which coincides with the onset of significant declines <36 ka ago in Beringian bison, horse, brown bear, and mammoth populations, as well as in mammoth genetic diversity. It appears likely that the impacts and population declines are related events, although their precise nature remains to be determined.

1. Introduction

During the late Pleistocene, Beringia was largely an ice-free continental region that consisted of northeastern Siberia, northwestern North America, and the emerged Bering Strait. Major events that occurred at that time were global climate changes, migration of humans from Asia to America (~13 ka BP), and large-scale megafaunal extinctions (~12 ka BP). The cause of these extinctions has long been controversial and has been attributed predominantly to either climate change or overkill by humans [*Martin*, 2005]. A period of marked decline in population and genetic diversity for many large mammal species happened earlier, however, beginning at about 36 ka BP before the last glacial maximum, human entry into the New World, or the final megafaunal extinctions. For instance, no brown bear fossils have been found in eastern Beringia (Alaska) that date between 35 and 21 ka BP, and different haplotypes at either end of this hiatus likely indicate a local extinction event [*Barnes et al.*, 2002]. Similarly, between 35 and 28 ka BP, caballoid horse fossils show a significant decline in metacarpal size and a coeval drop in the number of dated specimens, possibly reflecting lower population numbers,

and Alaskan wild asses apparently were extinct by ~31 ka BP [*Guthrie*, 2003]. The genetic diversity of Beringian Steppe bison dropped sharply after ~37 ka BP [*Shapiro et al*., 2004], and one of two major mammoth mitochondrial lineages also disappeared around this time [*Barnes et al*., 2007].

The final extinctions of megafauna were apparently contemporaneous with the abrupt onset of Younger Dryas cooling and termination of Clovis culture in North America. A carbon-rich black layer or "mat" lying above both megafaunal fossils and Clovis tools has been identified at over 50 sites across North America, which dates to ~12.9 ka BP [*Haynes*, 2005]. Directly beneath the black-mat horizon, *Firestone et al*. [2007] have found, at a number of places, a thin magnetic layer (<5 cm) containing magnetic particles, iridium, charcoal, soot, carbon microspherules, glass-like carbon containing nanodiamonds, and fullerenes with extraterrestrial helium. *Firestone et al*. [2007] have proposed that one or more extraterrestrial objects collided with and/or exploded over northern North America at this time leading to intense biomass burning. In addition, large spikes in ammonium and nitrate contents in layers of the Greenland GISP2 ice core at the beginning of the Younger Dryas are consistent with massive biomass burning at ~12.9 ka BP.

In this report we present preliminary evidence that supports a link between the ~36 ka BP decline in Beringian megafaunal populations and genetic diversity, and an extraterrestrial accretion event. Seven Alaskan mammoth tusks and one Siberian bison skull have been found with small magnetic (Fe-rich) particles embedded in them. We have radiocarbon dated the tusks and skull, and subjected the embedded magnetic particles to a battery of non-destructive tests to determine their chemical compositions and their possible origin as micrometeorites.

2. Analytical methods

To the naked eye, the dark particles embedded in the Alaskan mammoth tusks, and Siberian bison skull, appear to be composed of an oxidized metallic material. Upon closer inspection, the particle sites may or may not have raised rims, concentric "burn" rings, bulged centers, and/or "entry" pits (Fig. 1). Their attraction to a small neodymium magnet indicates that they are iron rich, and this quick and easy test was useful in sorting them from a large collection of fossils. The seven tusks and one skull with embedded particles are from a commercial supplier, and represent ~0.1% of the samples inspected at Canada Fossils, Ltd. Thus, no field notes documenting the source localities are available, and only general provenances can be assigned (Alaska or Siberia). Particles are found only on one side of any given fossil, and this is consistent with bombardment from a single direction. An X-ray image shows that the particles penetrated the tusks, presumably at high velocity, forming 2 to 5 mm diameter hemispherical debris patterns (Fig. 2). Sectioning and polishing of tusk/particle samples below (≤1 mm) the zone of concentrated debris show many small particles (<20 μm diameter) widely dispersed within the tusk matrix. The number and fundamental complexity of the embedded particles suggest that they are the result of a natural explosive event, and determining their chemical compositions is key to discovering their origin and the nature of this ancient event.

We analyzed particles extracted from six of the tusks and bison skull with laser ablation inductively coupled plasma mass spectrometry (LA-ICP-MS). In particular, we determined Ni/Fe ratios, as these are diagnostic of meteoritic and terrestrial compositions. Our results are given in Table 1, which also includes, for comparison, values for a variety of extraterrestrial and terrestrial samples. These analyses confirm the high Fe content of the particles and indicate compositions highly enriched in Ni and depleted in Ti, unlike any terrestrial values. A particle from tusk 1 also has a Ti/Fe ratio of 0.004, which is 3% of terrestrial values and comparable to those for CI chondrites. From X-ray fluorescence (XRF) analyses, we determined that the composition of the Fe-rich particles varies between native Fe, FeS, and FeO (Fig. 3), all typical of meteoritic compositions. Particles from tusks 2 and 3 are highly enriched in Ni (Table 1), and electron microprobe (EMP) analyses of a Fe-Ni sulfide grain from tusk 2 (Table 2) show two different phases within the grain that each contain Ni contents averaging 3 and 20 weight percent, respectively.

Particles embedded in the bison skull appear more angular (Fig. 4) than those embedded in the tusks (Fig. 1). Prompt Gamma-ray Activation Analysis (PGAA) of a particle extracted from the bison skull indicates that it contains 0.36 mg of iron, an amount consistent with an impacting particle ~1 mm in diameter. Furthermore, scanning electron microscope (SEM) images and XRF analyses of a broken section of bison skull show possible entry channels with straight sharp edges that contain Fe-rich material within them (Fig. 5).

Samples from all but one of the tusks, and bison skull, were submitted for ^{14}C dating to radiocarbon laboratories at the University of Arizona and the University of California at Irvine (Table 3). Samples from tusk 1 were dated twice at Arizona and once at UC Irvine. In general, the calibrated ages range between 31 and 36 ka with three exceptions: tusk 2 has an age of 20.1 ± 0.4 ka, the bison skull has an age of 26.3 ± 0.2 ka, and tusk 7 has an assigned age of >47.5 ka. The samples from tusk 2 and the bison skull might have been contaminated with younger carbon, and no detectable ^{14}C in tusk 7 indicates that it is radiocarbon "dead". Additional samples from these three specimens need to be dated. A weighted mean average for the 5 tusks with similar ages is 32.9 ± 0.2 ka. The 1σ error estimate for this overall mean is based only on laboratory error and, therefore, is probably too low. The range in ages for the three repeat measurements on tusk 1 is 3.6 ka or ± 1.8 ka, and is a better estimate of the true error.

3. Discussion of results

The high Ni concentrations and other Fe and sulfide compositions measured in the particles extracted from seven Alaskan mammoth tusks, and a Siberian bison skull, are in agreement with meteoritic compositions. Ni is relatively rare at the Earth's surface, and it is difficult to imagine any terrestrial process that would concentrate it within late Pleistocene fossils. Moreover, the particles are highly fragmented and appear to have exploded upon impact within the tusks. The apparent entry channels filled with Fe-rich material and more angular particles in the bison skull are consistent with impact into more porous and much softer bone, compared to the tooth-like hardness of tusks. In addition, the embedded particles are found only on one side of the fossils indicating that the particles arrived from a single direction, as they would from a micrometeorite shower.

Micrometeorites traveling at hypervelocities, however, cannot penetrate the Earth's atmosphere and reach the surface at high velocity due to atmospheric drag. Thus, we believe that the particles most likely arrived from an airburst, or from multiple airburst events over Beringia at around 33 ± 2 ka (perhaps similar to the 1908 Tunguska event), which locally pushed the atmosphere aside allowing the particles to travel greater distances at high velocity. Multiple airbursts would appear more likely due to the large area (several thousand km across) from which these fossils were recovered. Large-body impacts also produce high-speed ejecta particles, but these consist primarily of target material having terrestrial compositions. The 33 ± 2 ka age of the impacted fossils agrees with the onset of Beringian population declines around 36 kyr ago that has been documented from the fossil record [*Barnes et al*., 2002, 2007; *Guthrie*, 2003; *Shapiro et al*., 2004]. These declines preceded major megafaunal extinctions and the onset of Younger Dryas cooling in Beringia at ~12.9 ka, which also has been associated with an accretionary event [*Firestone et al*., 2007].

Sithylemenkat Lake is at the bottom of a topographic bowl-shaped depression in central Alaska (Fig. 6) and might be an impact crater also related to the 33 ka micrometeorite event. Located at 66.117°N and 151.383°W, the depression is 12.4 km in diameter and 500 m deep. Found during a search of Alaskan Landsat imagery for possible impact features, the Sithylemenkat Lake depression was selected because of its shape, and also because it is located in terrain unsuited for the formation of circular periglacial lakes or volcanic centers [*Cannon*, 1977]. Analysis of aerial photographs of the basin shows radial and concentric fractures similar to those associated with other known impact structures. Glacial features are absent within the basin indicating that it was not formed by glacial action and that it is probably late-to-post Wisconsin in age (<100 ka). Sediments from streams peripheral to the basin contain high Ni concentrations of up to 5000 ppm [*Herreid*, 1969] consistent with an impact, although ultramafic bedrock in the vicinity could be the source of the nickel. In addition, a pronounced aeromagnetic low is centered over the depression [*USGS*, 1973], and these are commonly associated with other large impact structures due to the intense fracturing of bedrock immediately below the crater floor [*Cannon*, 1977].

4. Conclusions

We propose that the metallic particles found embedded in late Pleistocene mammoth tusks and bison skull (assuming an incorrect age) are micrometeorites from low-level airbursts that occurred over Beringia sometime between 31 to 35 kyr ago. The result of these impacts likely caused the death of these seven Alaskan mammoths and one Siberian bison, as well as the overall decline in megafaunal populations observed throughout Beringia [e.g., *Shapiro et al*., 2004; *Barnes et al*., 2007]. Another of these meteors might have penetrated the atmosphere intact and formed the Sithylemenkat Lake crater in central Alaska.

As our sample population is small, the next step in our investigation is to contact and/or visit museums throughout North America and Siberia having collections of late Pleistocene Beringian fossils to see if we can discover more fossils embedded with micrometeorites. Also, an expedition to Sithylemenkat Lake crater is needed to collect

geologic samples and confirm the proposed extraterrestrial origin and age of this topographic feature.

Acknowledgements

The LA-ICP-MS and PGAA analyses were made at the Institute of Isotopes in Budapest, Hungary. We thank the technical staff there for their assistance in making these measurements. Also, we are grateful to Robert Oscarson at the USGS in Menlo Park, CA, for his assistance in making the SEM images, and the XRF and EMP analyses.

References

Barnes, I., P. Matheus, B. Shapiro, D. Jensen, A. Cooper, Dynamics of Pleistocene population extinctions of Beringian brown bears, *Science*, 295, 2267-2270 (2002),

Barnes, I., B. Shapiro, A. Lister, T. Kuznetsova, Andrei Sher, D. Guthrie, M.G. Thomas, Genetic structure and extinction of the woolly mammoth, *Mammuthus primigenius*, *Current Biology*, 17, 1072-1075 (2007).

Cannon, P.J., Meteorite impact crater discovered in central Alaska with Landsat imagery, *Science*, 196, 1322-1324 (1977).

Firestone, R.B., et al., Evidence for an extraterrestrial impact 12,900 years ago that contributed to the megafaunal extinctions and the Younger Dryas cooling, *Proc. Nat. Acad. Sci.*, 104, 16016-16021 (2007).

Firestone, R., A. West, S. Warwick-Smith, *The Cycle of Cosmic Catastrophes*, Bear & Company, Rochester, Vermont, 392 p. (2006).

Guthrie, R. D., Rapid body size decline in Alaskan Pleistocene horses before extinction, *Nature*, 426, 169-171 (2003).

Haynes, C. V., Jr., Clovis, Pre-Clovis, climate change, and extinction, in *Paleoamerican Origins: Beyond Clovis*, Bonnichsen, R., B. T. Lepper, D. Sanford, M. R. Waters, Eds., Texas A&M Univ. Press, College Station, Texas, 113-132 (2005)

Herreid, G., Geology and geochemistry, Sithylemenkat Lake area, Bettles Quadrangle, Alaska, *Alaska Div. Mines Geol. Rep. 35*, 22 p. (1969).

Martin, P.S., *Twilight of the Mammoths*, University of California Press, Berkeley, CA, 250 p., 2005.

Shapiro, B., et al., Rise and fall of the Beringian Steppe Bison, *Science*, 306, 1561-1565 (2004).

U.S. Geological Survey, Aeromagnetic survey, eastern part of Bettles quadrangle, northeast Alaska, *Open-File Report 73-305* (1973).

Table 1. Comparisons of Ni/Fe ratios between particles and meteoritic compositions

Sample	$(Ni/Fe)/(Ni/Fe)_{Terrestrial}$	Sample	$(Ni/Fe)/(Ni/Fe)_{Terrestrial}$
Tusk 1	6.4	Iron meteorite	110
Tusk 2	415	CI Chondrite	51
Tusk 3	190	H Chondrite	67
Tusk 4	10	K-T (Danish)	28
Tusk 5	22	Urelite	6
Tusk 6	5.6	Carb. Chondrite	3
Bison	8.5	Laurentian basalt	0.7

Notes: Ni/Fe ratios normalized by a bulk terrestrial value. K-T (Danish) indicates a sample from the Cretaceous-Tertiary boundary layer at Stevns Klint in Denmark.

Table 2. Microprobe data for a particle from Tusk 2

Site	S	Ni	Fe	Total
1 (red-org)	37.148	15.409	39.757	92.314
2 (gray)	15.402	4.777	46.796	66.975
3 (red-org)	40.850	20.727	32.726	94.303
4 (gray)	3.151	0.816	52.382	56.349
5 (red-org)	39.913	24.129	30.591	94.651
6 (gray)	12.810	4.328	49.392	66.530
Red-org avg.	39.304	20.088	34.358	93.756
Gray avg.	10.454	3.307	49.523	63.285

Notes: Under plain light, the particle appeared to be a mixture of two phases: one phase with a reddish-orange hue, and the other grayish in color. Compositional values are reported in weight percent. Totals do not sum to 100% indicating that other elements are present (Fig. 3c, d). Bottom two entries are averages (avg.) for each phase.

Table 3. ^{14}C dates for Mammoth tusks and Bison skull

Sample	Age	Error	Lab	Lab No.
Tusk 1	34479	323		
	33050	*520*	Arizona	AA63886
	36600	*2300*	Arizona	AA64879
	35340	*420*	UC Irvine	29597
Tusk 2	20960*	350	Arizona	AA64881
Tusk 3	31800	1300	Arizona	AA64880
Tusk 4	31250	330	UC Irvine	36479
Tusk 5	32030	360	UC Irvine	36480
Tusk 7	>47500*		UC Irvine	36481
Tusk 8	34510	500	UC Irvine	36482
Bison	26310*	150	UC Irvine	29596
Mean	32870	179	N = 5	

Notes: Tusk 1 was dated twice at the University of Arizona radiocarbon lab, and once at the UC Irvine lab (italics); a weighted mean of the three dates is given first. Tusk 6 has not been dated, and Tusk 7 has no detectable ^{14}C and is considered radiocarbon "dead". *, values omitted from weighted mean.

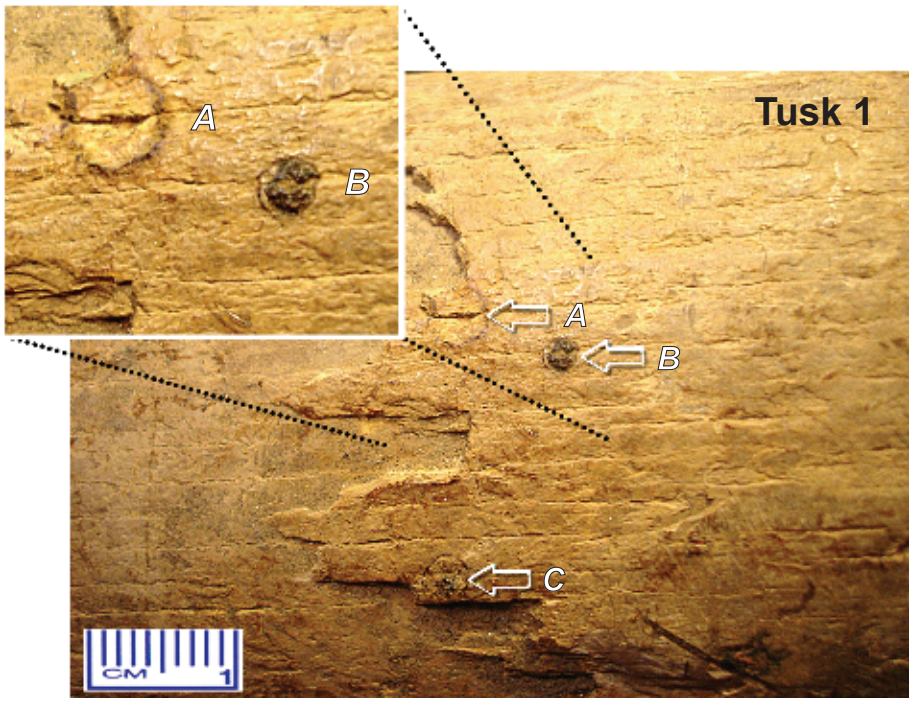

Figure 1. Close-up photograph and enlagement of metallic particles embedded in tusk 1. Several features can be seen associated with these particles; raised rim (*A*), "burn" ring (*B*, *C*), and bulged center (*B*).

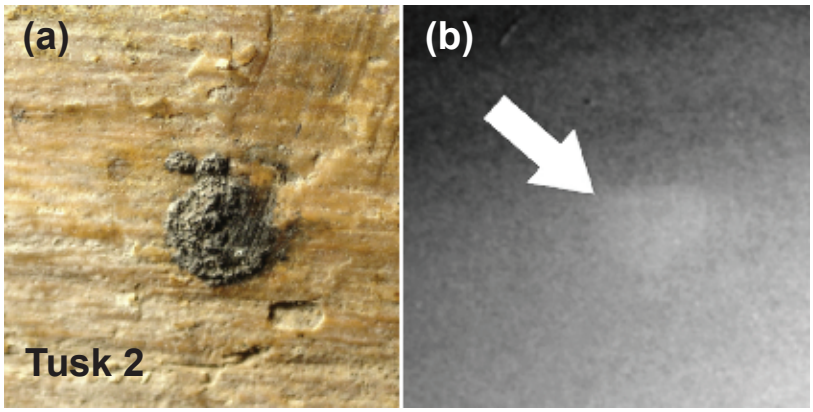

Figure 2. (a) Close-up photograph of a particle embedded in tusk 2. (b) X-ray image of the same particle in cross section showing hemispherical debris pattern. This particle is about the same size as particle *B* in Fig. 1.

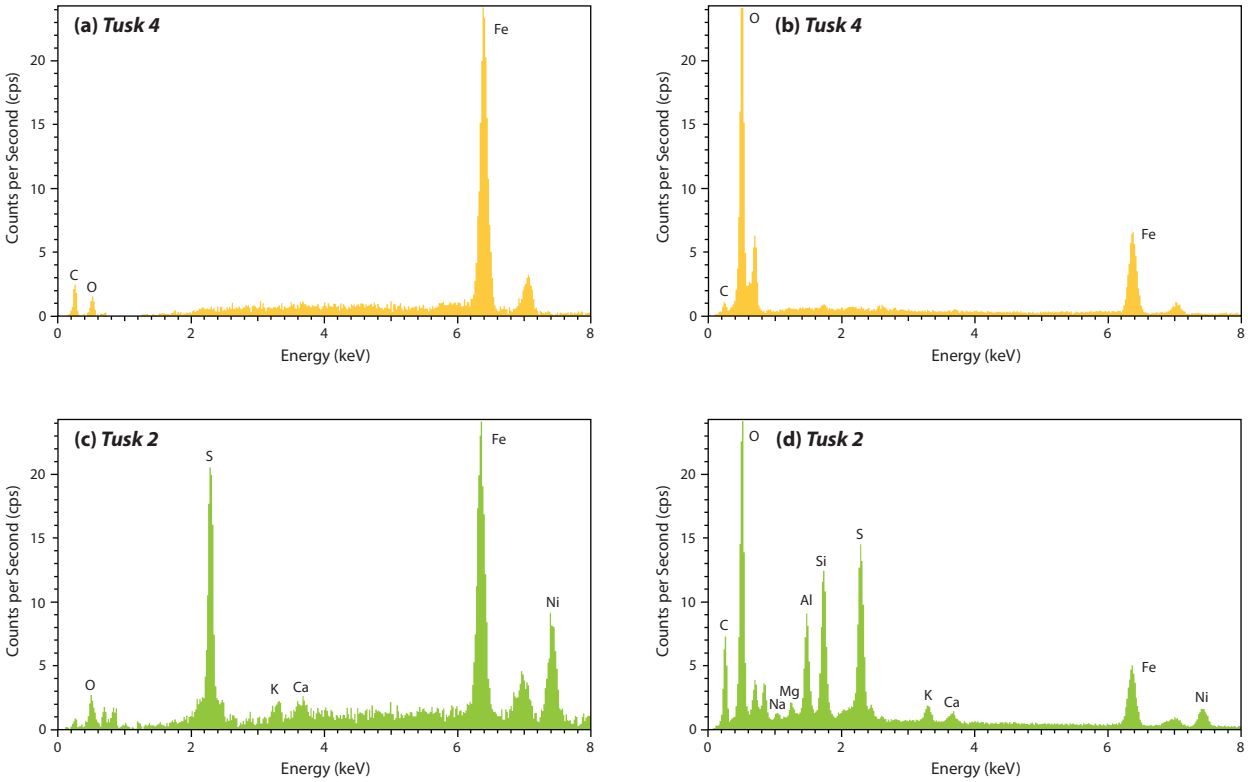

Figure 3. X-ray fluorescence (XRF) spectra showing the compositional variability within and between particles from two different tusks. Compositions range between native Fe (a), FeO (b), FeNiS (c, d). Silicate compositions in d are probably due to contamination from host sediments during burial.

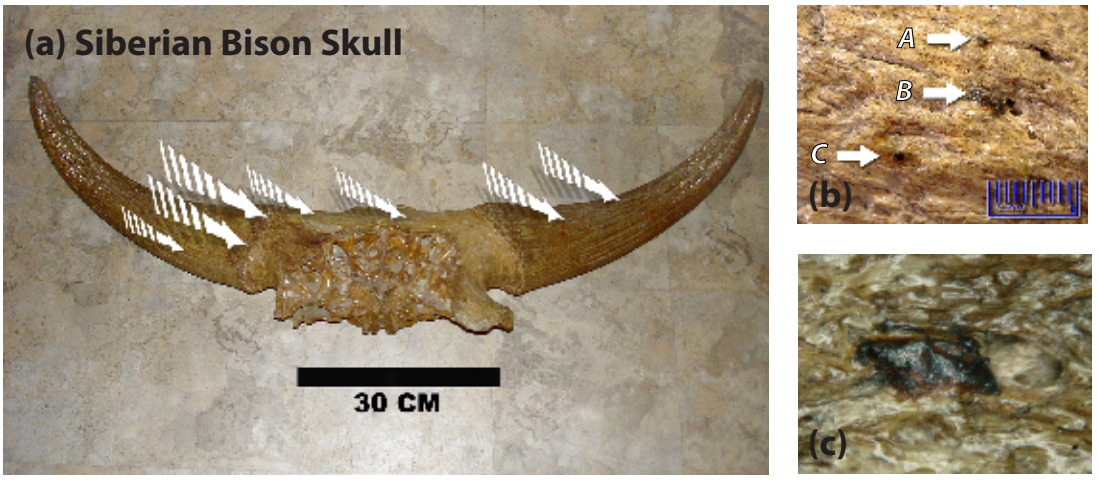

Figure 4. (a) Photograph of Siberian bison skull showing general locations of embedded metallic particles. (b) Close up photograph of particles in bison skull, and (c) enlargement of partcle about the size of particle *B* in b. Embedded particles in the bison skull appear more angular than those found in the tusks (Figs. 1, 2).

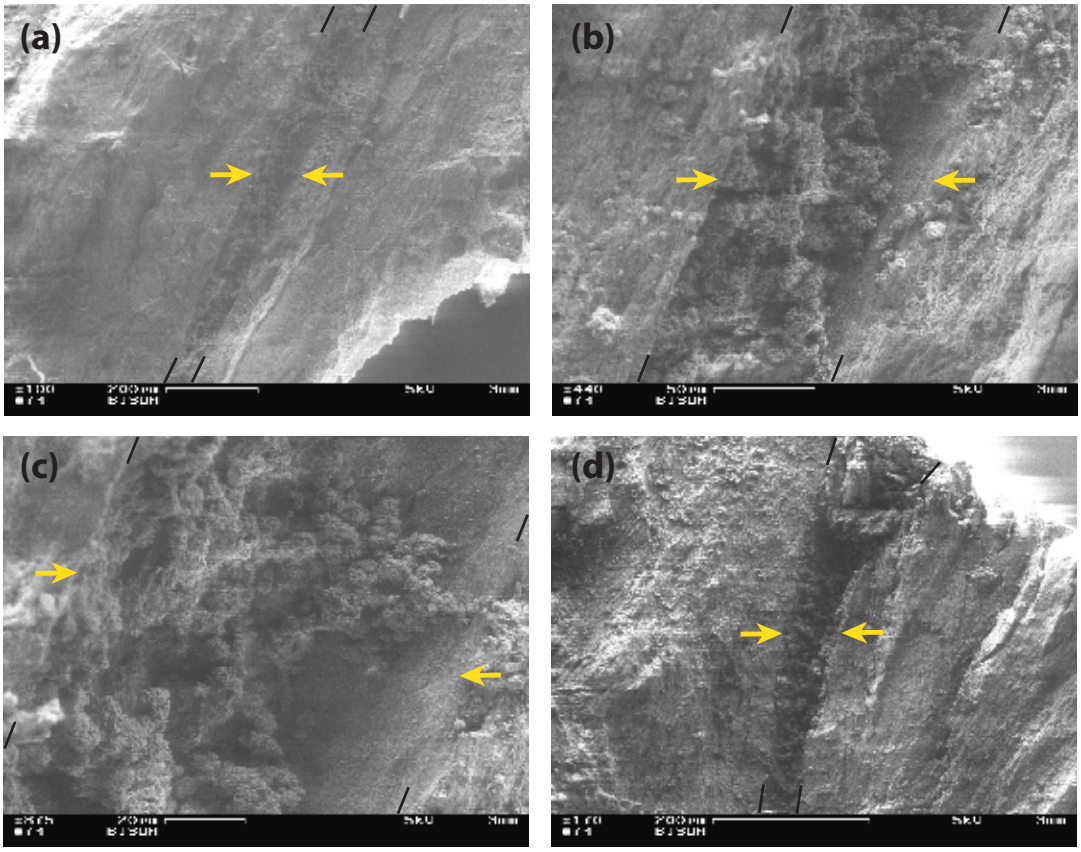

Figure 5. Scanning electron microscope (SEM) images of a cross section of the bison skull. The particles appear to have formed straight channels (a-c) where particle shards penetrated the bone. Clusters of iron particles at greatest enlargement (c) are seen inside the channel. A second channel is also shown (d). Black line segments and arrows indicate channel walls.

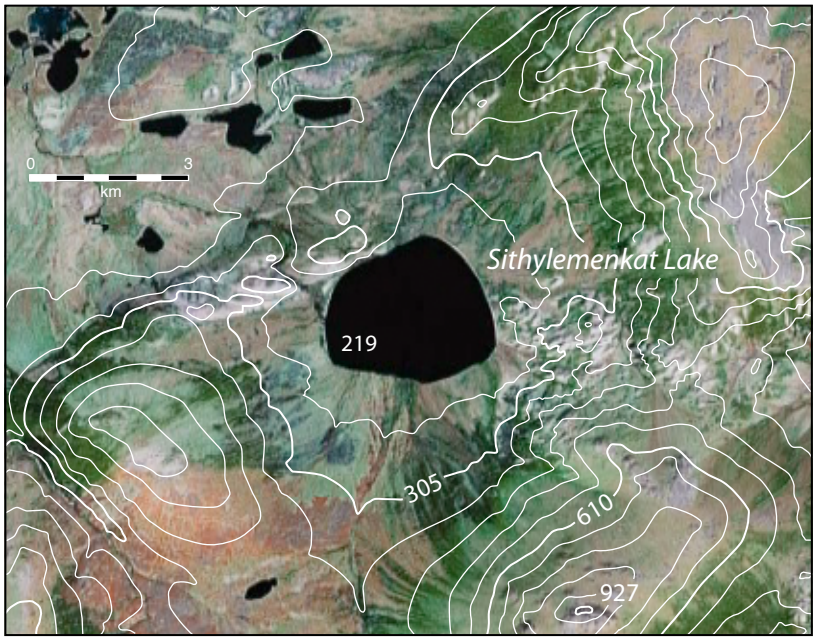

Figure 6. Sithylemenkat Lake (66.117°N, 151.383°W) at the bottom of a bowl-shaped topographic depression in central Alaska. Contour interval is 30.5 m (100 ft) and the level of the lake is at 219 m (720 ft).